

# Interband spectroscopy of Landau levels and magnetoexcitons in bulk black phosphorus

H. Okamura,<sup>1,\*</sup> S. Iguchi,<sup>2</sup> T. Sasaki,<sup>2</sup> Y. Ikemoto,<sup>3</sup> T. Moriwaki,<sup>3</sup> and Y. Akahama<sup>4</sup>

<sup>1</sup>*Department of Applied Chemistry, Tokushima University, Tokushima 770-8506, Japan*

<sup>2</sup>*Institute for Materials Research, Tohoku University, Sendai 980-8577, Japan*

<sup>3</sup>*Japan Synchrotron Radiation Research Institute, Sayo 679-5198, Japan*

<sup>4</sup>*Graduate School of Materials Science, University of Hyogo, Hyogo 678-1297, Japan*

(Dated: October 8, 2024)

Low-dimensional systems based on black phosphorus (BP) have recently attracted much interest. Since the crystal structure of BP consists of 2D layers with a strong in-plane anisotropy, its electronic properties at a high magnetic field ( $B$ ) are quite interesting. Here, we report a magneto-optical study of bulk BP at high  $B$  to 12 T perpendicular to the 2D layers. In the obtained optical conductivity spectra, periodic peaks are clearly observed corresponding to Landau levels of up to  $n=6$  quantum number. They exhibit almost linear shifts with  $B$ , and from their analysis an electron-hole reduced mass of  $0.13 m_0$  is obtained, where  $m_0$  is the electron mass. Many of the peaks appear in pairs, which is interpreted in terms of Zeeman splitting and an electron-hole combined  $g$ -factor of 6.6 is obtained. In addition, magnetoexciton peaks are observed to shift quadratically with  $B$ , and the exciton binding energy at  $B=0$  is estimated to be 9.7 meV.

## I. INTRODUCTION

Black phosphorus (BP) is one of the allotropes of phosphorus, which has a layered crystal structure with orthorhombic symmetry at ambient condition [1, 2]. As illustrated in Fig. 1(a), the structure consists of layers of P atoms formed by covalent bonding. The P atoms form a puckered, or the so-called “arm chair”, pattern along the  $x$  axis and a zigzag pattern along the  $y$  axis. The layers are stacked along the  $z$  axis by van der Waals bonding with a spacing of 5.3 Å. Although BP was first reported in 1914 [3], it was only after the successful synthesis of large single crystals in the 1980s [4, 5] that its physical properties were fully investigated [6–12]. At ambient condition, BP is a narrow-gap semiconductor with a band gap of 0.33 eV. According to band calculations [13–15] the minimum band gap is a direct gap located at the  $Z$  point of the Brillouin zone. An optical transition across the band gap is dipole allowed for polarization along the  $x$  axis but forbidden for that along the  $y$  axis [14, 15], resulting in large in-plane optical anisotropies as confirmed by experiment [16]. Recently, a successful realization of phosphorene [17, 18], namely an atomically thin layer of exfoliated BP, has led to a tremendous amount of research on BP-based low-dimensional systems [19]. In particular, the ability to tune the band gap [15, 20, 21] with the layer number makes phosphorene quite attractive for practical device applications [19]. Another remarkable feature of BP is a rich variety of phenomena induced by applying a high magnetic field [22–30], a high pressure [8, 9, 31, 32], and both of them [33–35]. The present work focuses on the electronic properties of bulk BP under high magnetic field ( $B$ ) probed by interband optical spectroscopy.

The electrons at high  $B$  undergo a cyclotron motion and their energy spectrum is quantized into discrete Landau levels (LLs). In a 2D electronic system this Landau quantization leads to the quantum Hall effect in transport proper-

ties [36], which was initially studied in semiconductor heterostructures and later in other 2D systems such as graphene [37, 38] and phosphorene [22]. The quantization may also be directly observed on the energy axis by a magneto-optical study, either by an intraband spectroscopy such as cyclotron resonance [39] or by an interband spectroscopy such as optical absorption/reflection and photoluminescence [40]. The properties of LLs and cyclotron motion in the highly anisotropic 2D layers of BP are quite interesting, and have motivated a large number of theoretical studies [23–29]. For example, unconventional  $B$  dependences of LL energies and optical selection rules have been predicted for few-layer and thin-film BPs [24, 25]. Rather surprisingly, however, there have been much fewer experimental reports on the magneto-optical properties of BP [7, 30] compared with the theoretical ones. For example, cyclotron resonance studies of bulk BP [7] were made soon after large single crystals became available. More recently, an ultrafast laser spectroscopy of bulk BP was made to study effects of magnetic fields on the anisotropic electron dynamics [30]. Nevertheless, magneto-optical properties of BP remain largely unexplored experimentally, and providing more magneto-optical data on BP should be essential for further development of BP research.

In this work, we have used an interband magnetoreflexion technique to probe the intriguing electronic properties of bulk BP at high  $B$  perpendicular to the 2D layers. In this technique, the optical reflectivity spectrum [ $R(\omega)$ ] of a sample measured at high  $B$  exhibits periodic peaks corresponding to interband transitions between LLs in valence and conduction bands. Alternatively,  $R(\omega)$  at a fixed  $\omega$  may be measured as a function of  $B$ . This technique has been applied to study LLs in various narrow-gap semiconductors and semimetals including Bi [41, 42] and graphite [43, 44]. Similarly, interband absorption has also been measured to probe, for example, LLs and Dirac states in graphene [45]. An advantage of these interband techniques is that the LLs can be observed even in the absence of excess carriers. We have clearly observed periodic peaks due to LL formation in  $R(\omega)$  of bulk BP at  $B \geq 5$  T, which shift almost linearly with  $B$ . The peak shifts seem to show conventional  $B$  dependence in spite of the large in-plane anisotropy.

\* Electronic address: ho@tokushima-u.ac.jp

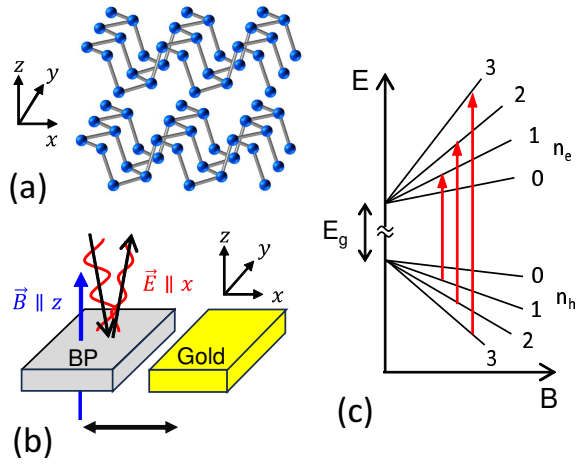


FIG. 1. (a) Crystal structure of BP at ambient condition [1, 2]. The  $x$  axis is along the so-called ‘‘arm chair’’ direction. (b) The configuration of sample and gold reference in the reflectivity study. External magnetic field ( $\vec{B}$ ) is applied along the  $z$  axis and the incident light is polarized ( $\vec{E}$ ) along the  $x$  axis. (c) A schematic diagram for LL formation as discussed in the text.  $E$  represents the electron energy, and  $E_g$  the band gap. (For simplicity, Zeeman splitting is omitted here.) The red arrows indicate interband optical transitions between LLs with the same quantum number,  $n_e = n_h$ .

From the data, the electron-hole reduced mass and effective  $g$ -factor are obtained. In addition, we have clearly identified magnetoexciton peaks and the exciton binding energy is obtained.

## II. EXPERIMENTAL METHODS

The samples of BP used in this work were grown by a high-pressure synthesis as described elsewhere [5]. A freshly cleaved sample surface containing the  $xy$  plane was used.  $R(\omega)$  spectra of the sample at high  $B$  were measured at the magneto-optics endstation [46] of the infrared beamline BL431R at SPring-8 [47] using synchrotron radiation as a bright infrared source [48]. Magnetic fields up to 14 T were generated by a superconducting magnet equipped with an infrared microscope. A BP sample and a gold reference mirror were mounted on the cold finger of a liquid He continuous-flow cryostat with a KBr optical window, which was inserted into the magnet bore. At each  $B$ , a measured reflection spectrum of the sample was divided by that of the gold to obtain the reflectivity,  $R(\omega)$ . The spectra were recorded with an FTIR spectrometer and a HgCdTe detector. As illustrated in Fig. 1(b), the measurements were made under a Faraday geometry, where  $\vec{B}$  was applied perpendicular to the sample surface ( $xy$  plane) and  $R(\omega)$  was measured under a near-normal incidence. The incident light was polarized along the  $x$  axis, which leads to dipole-allowed direct transitions across the band gap.

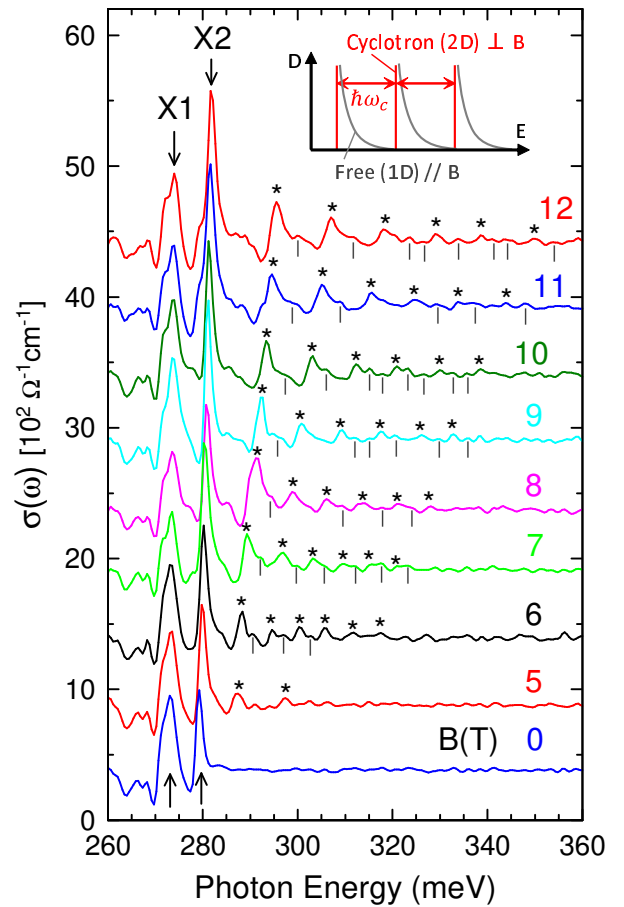


FIG. 2. Optical conductivity [ $\sigma(\omega)$ ] spectra of bulk BP measured at 12 K under high magnetic field ( $B$ ) exhibiting periodic peaks due to LL formation. Each spectrum is vertically offset by  $500 \Omega^{-1} \text{cm}^{-1}$  for clarity. The asterisks and vertical bars indicate main peaks and subpeaks, respectively, discussed in the text. The vertical arrows indicate exciton peaks X1 and X2. The inset illustrates the electron density of states ( $D$ ) versus energy ( $E$ ) at high  $B$ .  $\hbar\omega_c$  denotes the cyclotron energy.

## III. RESULTS AND DISCUSSIONS

Figure 2 indicates the optical conductivity [ $\sigma(\omega)$ ] of bulk BP measured at 12 K and at different  $B$  to 12 T over a spectral range in which the band gap is located. They have been obtained from the measured  $R(\omega)$  spectra, which are indicated in Supplemental Material [49], using the Kramers-Kronig analysis [50, 51]. It is seen that the spectral shapes of  $\sigma(\omega)$  are very similar to those of the corresponding  $R(\omega)$ . At  $B=0$ , the main spectral features in  $\sigma(\omega)$  are the two peaks indicated by vertical arrows, which are located at 273.0 and 279.3 meV and labeled as X1 and X2, respectively. Later, it will be shown that the X1 and X2 peaks correspond to the ground and first excited states of exciton, respectively. (They would correspond to the  $1s$  and  $2s$  states, respectively, in case of a hydrogen-like exciton.) Except for these exciton peaks, the spectra are almost featureless at  $B=0$ . At  $B \geq 5$  T, however, multiple

peaks emerge as marked with the asterisks and vertical bars in Fig. 2. Note that the peaks with asterisks, which we hereafter refer to as the “main peaks”, appear periodic in energy and their energy interval increases with  $B$ . On the other hand, the peaks with vertical bars, which we refer to as the “subpeaks”, are weaker than the main peaks. The main peaks are much more clearly observed than the subpeaks. These periodic peaks are apparently associated with interband optical transitions between LLs formed in valence and conduction bands, as shown by Fig. 1(c) [40]. The optical transitions in Fig. 1(c) are indicated with the conventional selection rule (between LLs with the same quantum number), although some unconventional selection rules have been predicted for a few-layer BP [24] as discussed later. Note that bulk BP is not a completely 2D system since the interlayer electronic coupling is fairly strong [13–15]. Therefore, the energy dispersion along the  $z$  axis is continuous even when that along the  $xy$  plane is quantized by a magnetic field. Despite this, the measured  $\sigma(\omega)$  still exhibits a LL quantization because, for the 1D motion of electrons along  $z$ , the density of states ( $D$ ) decreases with energy ( $E$ ) as  $D \propto 1/\sqrt{E}$  as shown by the inset of Fig. 2.

To further analyze the data, the overall peak energies of  $\sigma(\omega)$  in Fig. 2 are plotted versus  $B$  in Fig. 3(a), where the main peaks and subpeaks are indicated by filled and empty circles, respectively. This so-called “fan plot” clearly shows the characteristic variation of transition energy with  $B$ . Pairs of main peak and subpeak, marked by  $n=1$  to 6, are observed to shift almost linearly with  $B$ . In addition, the interval between the main peak and subpeak is also increasing with  $B$ . These peaks exhibit much larger shifts with  $B$  than X1 and X2 peaks, which suggests different characteristics between the two groups of peaks. The former group of peaks should arise from free electron-hole pair creations and their linear  $B$  dependence is due to the increase of cyclotron energy. In a simple free-electron model, the LL energy spectra of electron ( $e$ ) and hole ( $h$ ) are expressed as  $\epsilon_{n,i} = (n_i + 1/2)\hbar\omega_{c,i}$ , where  $n_i = 0, 1, 2, \dots$  is the quantum number,  $\omega_{c,i}$  is the cyclotron energy, and  $i = e$  or  $h$  [40]. As already mentioned, interband transitions are allowed only between LLs with  $n_e = n_h$ , so the interband transition energy is expressed as

$$E = E_g + \left(n + \frac{1}{2}\right)\hbar\omega_c^* = E_g + \left(n + \frac{1}{2}\right)\left(\frac{\hbar e}{m_r^*}\right)B. \quad (1)$$

Here,  $E_g$  is the band gap,  $n = 0, 1, 2, \dots$ ,  $\omega_c^* = \omega_{c,e} + \omega_{c,h}$  is the combined cyclotron frequency, and  $1/m_r^* = 1/m_e^* + 1/m_h^*$  where  $m_r^*$  is the reduced effective mass, and  $m_e^*$  ( $m_h^*$ ) is the electron (hole) effective mass. Namely, the transition energy is expected to shift linearly with  $B$  and its slope should be given by  $(n + 1/2)\hbar e/m_r^*$ . Accordingly, a linear fitting of the form  $E = E_g + S \cdot B$  has been performed on the data in Fig. 3(a), where the slope  $S$  is a fitting parameter and  $E_g$  (the vertical intercept of the graph) is kept the same for all the peaks. It has been found that the best overall fitting is obtained when  $E_g$  is in the range  $282.7 \pm 0.5$  meV. The result of fitting with  $E_g = 282.7$  meV is indicated by the colored straight lines in Fig. 3(a). Note that the band gap of bulk BP at 12 K obtained here,  $E_g = 282.7$  meV, is much smaller than that at room

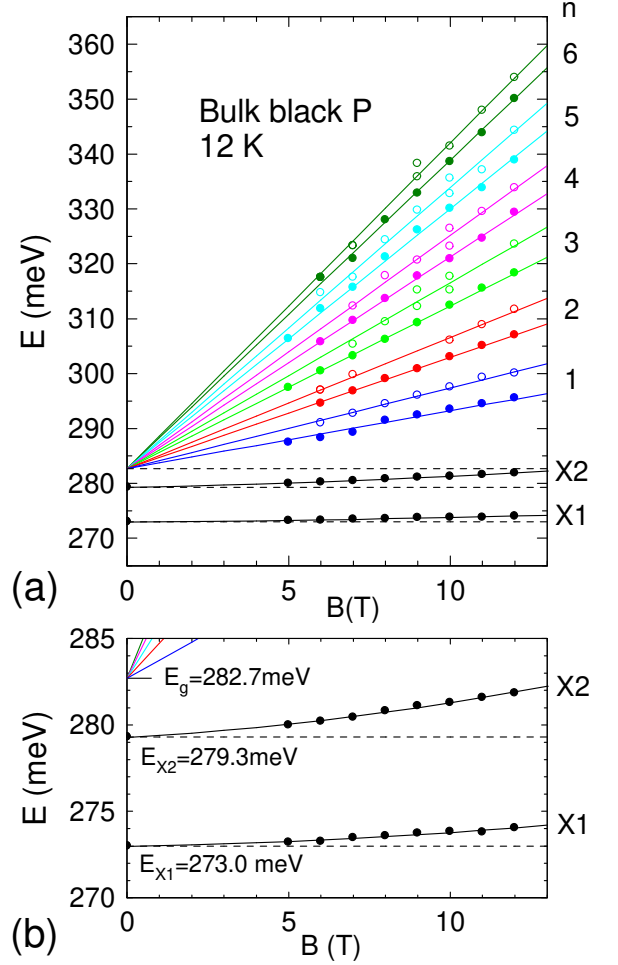


FIG. 3. (a) The energies ( $E$ ) of main peaks (colored filled circles) and subpeaks (empty circles), which are marked by asterisks and vertical bars in Fig. 2, respectively, and X1 and X2 peaks (black filled circles) plotted versus  $B$ . The colored lines indicate results of linear fitting to the peaks with  $n=1-6$  and the black curves those of quadratic fitting to X1 and X2 peaks. The horizontal broken lines are guide to the eye. (b) The  $B$  dependences of X1 and X2 peaks displayed on an expanded scale. The band gap ( $E_g$ ) estimated from the  $n=1-6$  peaks and the observed peak energies of X1 and X2 at  $B=0$  ( $E_{X1}$  and  $E_{X2}$ ) are also indicated.

temperature (330 meV) since  $E_g$  of bulk BP is significantly reduced by cooling [52].

The slopes obtained by the fitting in Fig. 3 are summarized in Table I and plotted versus  $n$  in Fig. 4. It is apparent from Table I that the observed values of  $S_n(\text{main})$ , namely the slope of the  $n$ th main peak, are close to multiples of  $S_1(\text{main})$ , which does not fit with the form of Eq. (1). Hence, we assume that each pair of adjacent main peak and subpeak results from the Zeeman splitting of a LL. Theoretically, more complicated splitting may be expected since the wavefunction around  $Z$  point should contain a strong  $p$  component [13, 14]. Namely, a spin-orbit coupling may split the  $p$  states into  $j=3/2$  and  $1/2$ , which may further split into  $m_j = \pm 3/2$

TABLE I. Slopes ( $S_n$ ) in units of meV/T obtained from the linear fitting to the peaks with  $n = 1 - 6$  and  $E_g=282.7$  meV in Fig. 3(a).  $S_n(\text{main})$  and  $S_n(\text{sub})$  indicate the slopes of the main peak and sub-peak, which are marked by the asterisks and vertical bars in Fig. 2, respectively.  $S_n(\text{mid})$  and  $\Delta S_n$  indicate the middle value of  $S_n(\text{main})$  and  $S_n(\text{sub})$  and the difference between them, respectively. The variation in  $S_n$  when  $E_g$  is varied by  $\pm 0.5$  meV is about  $\pm 0.5$  meV for the main peaks for all  $n$ .

$n$	1	2	3	4	5	6
$S_n(\text{main})$	1.05	2.03	2.96	3.85	4.73	5.61
$S_n(\text{sub})$	1.47	2.39	3.38	4.25	5.12	5.93
$S_n(\text{mid})$	1.26	2.21	3.17	4.05	4.93	5.77
$\Delta S_n$	0.42	0.36	0.42	0.39	0.39	0.32

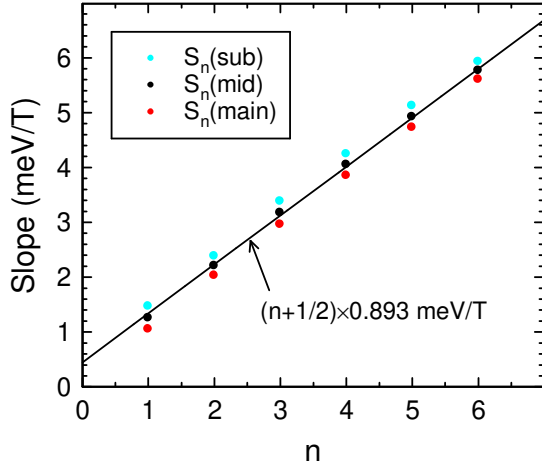


FIG. 4. Slopes of the main peak [ $S_n(\text{main})$ , red dots], sub-peak [ $S_n(\text{sub})$ , blue dots] and their middle value [ $S_n(\text{mid})$ , black dots] from Table I are plotted versus  $n$ . The solid line shows a linear fit to  $S_n(\text{mid})$ .

and  $\pm 1/2$  states at high  $B$ , where  $j$  and  $m_j$  are total angular momentum and magnetic quantum numbers, respectively [40]. In our data, however, such complicated splitting is not observed. We therefore assume phenomenologically a Zeeman splitting of the form  $E_n^\pm = E_n \pm \frac{1}{2}\Delta E_n$ , and assume that  $E_n^-$  and  $E_n^+$  correspond to the main peak and subpeak, respectively. Then, the middle value of  $S_n(\text{main})$  and  $S_n(\text{sub})$  should correspond to the slope of the  $n$ th LL. In Table I and Fig. 4, the middle values are indicated and denoted as  $S_n(\text{mid})$ . As indicated by the straight line in Fig. 4,  $S_n(\text{mid})$  can be fitted well as  $S_n(\text{mid}) = (n + \frac{1}{2}) \times 0.893$  meV/T. Namely, the  $B$  dependence of  $S_n(\text{mid})$  is consistent with Eq. (1). This result also shows that a LL peak with  $n=0$  is absent in the present data. It is unclear why an  $n=0$  peak is not observed here, but some kind of broadening may have wiped out the  $n=0$  peak. It is also unclear why the subpeak is much weaker than the main peak. The intensity of a peak in  $\sigma(\omega)$  should be proportional to the joint density of states (JDOS) and the transition probability ( $P$ ). In our simplified model, the main peak and

subpeak correspond to interband transitions ( $\epsilon_{n,h}^+ \rightarrow \epsilon_{n,e}^-$ ) and ( $\epsilon_{n,h}^- \rightarrow \epsilon_{n,e}^+$ ), respectively, where  $-$  and  $+$  symbols express the lower- and higher-energy Zeeman split levels, respectively [53]. Both JDOS and  $P$  should be the same for the two transitions. Therefore, other factors not considered here, such as a mixing among spin-orbit split states at high  $B$ , may have resulted in their different intensities.

Besides the absence of an  $n=0$  peak, the LL peak energies in Fig. 3(a) seems to follow a conventional  $B$  dependence of Eq. (1), despite the large in-plane anisotropy in BP. In the case of thin-film BPs, in contrast, unconventional selection rules such as  $n_e = n_h \pm 2$  and nonlinear shifts of LL peaks with  $B$  have been predicted as already mentioned [24]. Theoretically, similar results may be expected for a bulk BP at certain values of  $k_z$ , but again, it may not be observed in actual experiments [55]. Comparing  $S_n(\text{mid}) = (n + \frac{1}{2}) \times 0.893$  meV/T with Eq. (1),  $0.893$  meV/T should be equal to  $(\hbar e/m_r^*)$ , which yields  $m_r^* = 0.129 m_0$ . Previous cyclotron resonance study of  $n$ -type and  $p$ -type BP reported in-plane effective masses of  $m_e^* = 0.291 m_0$  and  $m_h^* = 0.222 m_0$  [7], which give a reduced effective mass of  $m_r^* = 0.126 m_0$ . Therefore, the present result of  $m_r^* = 0.129 m_0$  is very close to the cyclotron resonance result. In our interpretation of the data,  $\Delta S_n = S_n(\text{sub}) - S_n(\text{main})$  should be equal to  $\Delta E_n/B$ . Since  $\Delta E = g^* \mu_B B$ , where  $g^*$  is the  $e$ - $h$  combined effective  $g$ -factor and  $\mu_B$  is the Bohr magneton,  $\Delta S_n = g^* \mu_B$ . This relation and the average of  $\Delta S_n$  from Table I,  $0.384$  meV/T, yields  $g^* = 6.6$ . A theoretical study has estimated the electron effective  $g$ -factor in bulk BP to be 3 [28], which is about one-half the present result. Since  $g^*$  obtained here contains both electron and hole contributions, our result of  $g^* = 6.6$  seems quite reasonable in comparison with the theoretical estimate.

Now we look more closely into the  $B$  dependences of X1 and X2 peak energies, which are displayed in an expanded scale in Fig. 3(b). The solid curves in Fig. 3(b) indicate results of quadratic fitting of the form  $E(B) = aB^2 + bB + E_{X1,X2}$  to the data, where  $a$  and  $b$  are fitting parameters. The  $E(B)$  obtained with the fitting [56] has a strong  $B^2$  term comparable with the  $B$  term. Such a quadratic shift is a well-known property of magnetoexcitons [40, 57] and is often referred to as a diamagnetic shift. Note also that X2 peak exhibits much larger shifts with  $B$  than X1 peak. This is also a property of ground and excited states of magnetoexcitons [57]. From these results, we attribute X1 and X2 peaks to the ground and first excited states of exciton, respectively, which would correspond to the  $1s$  and  $2s$  states in case of a hydrogen-like exciton. As discussed above, the results on LL peaks have yielded  $E_g = 282.7 \pm 0.5$  meV. The exciton binding energy  $E_b$  should be given by the difference between  $E_g$  and  $E_{X1}$ , so we obtain  $E_b = 9.7 \pm 0.5$  meV. This is close to the theoretical estimate of  $9.1$  meV [54], which was obtained taking into account the large anisotropy of BP. For a hydrogen-like exciton, the energy separation between  $1s$  and  $2s$  states is  $\Delta E_{1s-2s} = (3/4)E_b$ . By setting  $E_b = 9.7$  meV, this would give  $\Delta E_{1s-2s} = 7.3$  meV. From the observed X1 and X2 peaks, on the other hand, their energy separation is  $\Delta E_{X1-X2} = 6.3$  meV and smaller than the  $(3/4)E_b$  value above. This disagreement is not surprising since the actual situation of excitons in bulk

BP is quite different from that of a hydrogen-like, isotropic exciton. Although the exciton energy in bulk BP has been considered for the ground state [54], further theoretical studies are needed for excited states and the  $B$  dependence of both ground and excited states to fully understand the properties of magnetoexcitons in bulk BP. In addition, our clear observation of magnetoexcitons in a bulk BP makes similar studies on few-layer and thin-film BPs quite appealing. Since the exciton binding energy should be much more enhanced than in the bulk [20, 21], magnetoexciton properties in a few-layer BP are quite intriguing. Furthermore, even more complex exciton states such as trions (*e.g.*, a charged exciton consisting of two electrons and a hole [58]) may be explored in few-layer BPs.

#### IV. SUMMARY

Infrared magnetoreflection study has been made on bulk BP single crystals at high  $B$  perpendicular to the 2D layers. At  $B \geq 5$  T, the obtained  $\sigma(\omega)$  spectra exhibit periodic peaks due

to interband transitions between LLs in conduction and valence bands. The peaks show linear shifts with  $B$ , which agree well with the standard form of  $E_n = E_g + (n + \frac{1}{2}) \hbar\omega_c^*$ . From the data, an electron-hole reduced mass of  $m_r^* = 0.129 m_0$  is obtained, which agrees well with that reported previously by a cyclotron resonance study. In addition, from the observed interval between the main peak and subpeak, an electron-hole combined effective  $g$ -factor of 6.6 has been obtained. Furthermore, magnetoexciton peaks with characteristic quadratic-in- $B$  shifts have also been observed, and the exciton binding energy at  $B=0$  is estimated to be  $9.7 \pm 0.5$  meV.

#### V. ACKNOWLEDGMENTS

The authors would like to thank Dr. X. Zhou for useful communications. The experiments at SPring-8 were performed under the approval by JASRI (2016A0073, 2017A1164, 2017B1389, 2018A1130). Financial support from Japan Society for the Promotion of Science (KAKENHI Grant No. 26400358) is acknowledged.

- 
- [1] A. Brown and S. Rundqvist, Refinement of the crystal structure of black phosphorus, *Acta Crystallogr.* **19**, 684 (1965).
- [2] The  $x$ ,  $y$ , and  $z$  directions here correspond to the crystallographic  $c$ ,  $a$ , and  $b$  axes, respectively [1].
- [3] P. W. Bridgman, Two new modifications of phosphorus, *J. Am. Chem. Soc.* **36**, 1344 (1914).
- [4] I. Shirovani, Growth of Large Single Crystals of Black Phosphorus, *Mol. Cryst. Liq. Cryst.* **86** (1982) 203.
- [5] S. Endo, Y. Akahama, S. Terada, and S. Narita, Growth of Large Single Crystals of Black Phosphorus under High Pressure, *Jpn. J. Appl. Phys.* **21**, L482 (1982).
- [6] Y. Akahama, S. Endo, and S. Narita, Electrical Properties of Black Phosphorus Single Crystals, *J. Phys. Soc. Jpn.* **52**, 2148 (1983).
- [7] S. Narita, S. Terada, S. Mori, K. Muro, Y. Akahama, and S. Endo, Far-Infrared Cyclotron Resonance Absorptions in Black Phosphorus Single Crystals, *J. Phys. Soc. Jpn.* **52**, 3544 (1983).
- [8] M. Okajima, S. Endo, Y. Akahama, and S. Narita, Electrical Investigation of Phase Transition in Black Phosphorus under High Pressure, *J. Jpn. Appl. Phys.* **23** 15 (1984).
- [9] H. Kawamura, I. Shirovani, and K. Tachikawa, Anomalous superconductivity in black phosphorus under high pressures, H. Kawamura, I. Shirovani, and K. Tachikawa, *Solid State Commun.* **49**, 879 (1984).
- [10] Early experiments performed on large single crystals of BP in 1980s have been summarized in A. Morita, *Semiconducting black phosphorus*, *Appl. Phys. A* **39**, 227 (1986).
- [11] Y. Akahama and S. Endo, Transport study on pressure-induced band overlapped metallization of layered semiconductor black phosphorus, *Solid State Commun.* **104**, 307 (1997).
- [12] Y. Akahama and H. Kawamura, Optical and Electrical Studies on Band-Overlapped Metallization of the Narrow-Gap Semiconductor Black Phosphorus with Layered Structure, *physica status solidi (b)* **223**, 349 (2001).
- [13] Y. Takao, H. Asahina, and A. Morita, Electronic Structure of Black Phosphorus in Tight Binding Approach, *J. Phys. Soc. Jpn.* **50**, 3362 (1981).
- [14] H. Asahina, K. Shindo, and A. Morita, Electronic Structure of Black Phosphorus in Self-Consistent Pseudopotential Approach, *J. Phys. Soc. Jpn.* **51**, 1193 (1982).
- [15] J. Qiao, X. Kong, Z.-X. Hu, F. Yang, and W. Ji, High-mobility transport anisotropy and linear dichroism in few-layer black phosphorus, *Nature Commun.* **5**, 4475 (2014).
- [16] F. Xia, H. Wang, and Y. Jia, Rediscovering black phosphorus as an anisotropic layered material for optoelectronics and electronics, *Nature Commun.* **5**, 4458 (2014).
- [17] L. Li, Y. Yu, G. J. Ye, Q. Ge, X. Ou, H. Wu, D. Feng, X. H. Chen, and Y. Zhang, Black phosphorus field-effect transistors, *Nature Nanotech.* **9**, 372 (2014).
- [18] H. Liu, A. T. Neal, Z. Zhu, Z. Luo, X. Xu, D. Tomanek, and P. D. Ye, Phosphorene: An Unexplored 2D Semiconductor with a High Hole Mobility, *ACS Nano* **8**, 4033 (2014).
- [19] For a review on the phosphorene research, see, for example, J. Miao, L. Zhang, and C. Wang, Black phosphorus electronic and optoelectronic devices, *2D Mater.* **6**, 032003 (2019).
- [20] L. Li, J. Kim, C. Jin, G. J. Ye, D. Y. Qiu, F. H. da Jornada, Z. Shi, L. Chen, Z. Zhang, F. Yang, K. Watanabe, T. Taniguchi, W. Ren, S. G. Louie, X. H. Chen, Y. Zhang, and F. Wang, Direct observation of the layer-dependent electronic structure in phosphorene, *Nature Nanotech.*, **12**, 21 (2017).
- [21] G. Zhang, S. Huang, A. Chaves, C. Song, V. O. Ozcelik, T. Low, and H. Yan, Infrared fingerprints of few-layer black phosphorus, *Nature Commun.* **8**, 14071 (2017).
- [22] L. Li, F. Yang, G.J. Ye, Z. Zhang, Z. Zhu, W. Lou, X.-Y. Zhou, Liang Li, K. Watanabe, T. Taniguchi, K. Chang, Y. Wang, X. Chen, and Y. Zhang, Quantum Hall effect in black phosphorus two-dimensional electron system, *Nature Nanotech.* **11**, 593 (2016).
- [23] X. Zhou, R. Zhang, J. P. Sun, Y. L. Zou, D. Zhang, W. K. Lou, F. Cheng, G. H. Zhou, F. Zhai, and Kai Chang, Landau levels and magneto-transport property of monolayer phosphorene, *Sci. Rep.* **5**, 12295 (2015).

- [24] X. Zhou, W.-K. Lou, F. Zhai, and K. Chang, Anomalous magneto-optical response of black phosphorus thin films, *Phys. Rev. B* **92**, 165405 (2015).
- [25] M. Tahir, P. Vasilopoulos, and F. M. Peeters, Magneto-optical transport properties of monolayer phosphorene, *Phys. Rev. B* **92**, 045420 (2015).
- [26] Y. Jiang, R. Roldan, F. Guinea, and T. Low, Magnetoelectronic properties of multilayer black phosphorus, *Phys. Rev. B* **92**, 085408 (2015).
- [27] J. M. Pereira, Jr. and M. I. Katsnelson, Landau levels of single-layer and bilayer phosphorene, *Phys. Rev. B* **92**, 075437 (2015).
- [28] X. Zhou, W.-K. Lou, D. Zhang, F. Cheng, G. Zhou, and K. Chang, Effective  $g$  factor in black phosphorus thin films, *Phys. Rev. B* **95**, 045408 (2017).
- [29] P. Wu, Z.-G. Shi, X. Chen, and X. Zhou, Anisotropic magneto-optical transport properties in black phosphorus induced by in-plane magnetic field, *J. Phys.: Condens. Matter* **35**, 065701 (2023).
- [30] X. Liu, W. Lu, X. Zhou, Y. Zhou, C. Zhang, J. Lai, S. Ge, M. C. Sekhar, S. Jia, K. Chang, and D. Sun, Dynamical anisotropic response of black phosphorus under magnetic field, *2D Mater.* **5**, 025010 (2018).
- [31] P. Di. Pietro, M. Mitrano, S. Caramazza, F. Capitani, S. Lupi, P. Postorino, F. Ripanti, B. Joseph, N. Ehlen, A. Gruneis, A. Sanna, G. Profeta, P. Dore, and A. Perucchi, Emergent Dirac carriers across a pressure-induced Lifshitz transition in black phosphorus *Phys. Rev. B* **98**, 165111 (2018).
- [32] For the development of high-pressure research on BP, see, for example, X. Li, J. Sun, P. Shahi, M. Gao, A. H. MacDonald, Y. Uwatoko, T. Xiang, J. B. Goodenough, J. Cheng, and J. Zhou, Pressure-induced phase transitions and superconductivity in a black phosphorus single crystal, *Proc. Nat. Acad. Sci.* **115**, 9935 (2018), and references cited therein.
- [33] K. Akiba, A. Miyake, Y. Akahama, K. Matsubayashi, Y. Uwatoko, and M. Tokunaga, Anomalous Quantum Transport Properties in Semimetallic Black Phosphorus, *J. Phys. Soc. Jpn.* **84**, 073708 (2015).
- [34] Z. J. Xiang, G. J. Ye, C. Shang, B. Lei, N. Z. Wang, K. S. Yang, D. Y. Liu, F. B. Meng, X. G. Luo, L. J. Zou, Z. Sun, Y. Zhang, and X. H. Chen, Pressure-Induced Electronic Transition in Black Phosphorus, *Phys. Rev. Lett.* **115**, 186403 (2015).
- [35] T. Fujii, Y. Nakai, M. Hirata, Y. Hasegawa, Y. Akahama, K. Ueda, T. Mito, Giant Density of States Enhancement Driven by a Zero-Mode Landau Level in Semimetallic Black Phosphorus under Pressure, *Phys. Rev. Lett.* **130**, 076401 (2023).
- [36] See, for example, K. von Klitzing, The quantized Hall effect, *Rev. Mod. Phys.* **58**, 519 (1986).
- [37] K. S. Novoselov, A. K. Geim, S. V. Morozov, D. Jiang, M. I. Katsnelson, I. V. Grigorieva, S. V. Dubonos, and A. A. Firsov, Two-dimensional gas of massless Dirac fermions in graphene, *Nature* **438**, 197 (2005).
- [38] Y. Zhang, Y.-W. Tan, H. L. Stormer, and P. Kim, Experimental observation of the quantum Hall effect and Berry's phase in graphene, *Nature* **438**, 201 (2005).
- [39] See, for example, D. J. Hilton, T. Arikawa, and J. Kono, Cyclotron Resonance, in *Characterization of Materials, 2nd Ed.*, edited by E. N. Kaufmann (Wiley, 2012).
- [40] See, for example, D. Heiman, Laser Spectroscopy of Semiconductors at Low Temperatures and High Magnetic Fields, *Semiconductors and Semimetals Vol. 36*, edited by D. G. Seiler and C. L. Littler (Academic Press, Boston, MA, 1992), Chap. 1.
- [41] M. P. Vecchi, J. R. Pereira, and M. S. Dresselhaus, Anomalies in the magnetoreflection spectrum of bismuth in the low-quantum-number limit, *Phys. Rev. B* **14**, 298 (1976).
- [42] A. A. Schafgans, K. W. Post, A. A. Taskin, Y. Ando, X.-L. Qi, B. C. Chapler, and D. N. Basov, Landau level spectroscopy of surface states in the topological insulator  $\text{Bi}_{0.91}\text{Sb}_{0.09}$  via magneto-optics, *Phys. Rev. B* **85**, 195440 (2012).
- [43] W. W. Toy, C. R. Hewes, and M. S. Dresselhaus, Magnetoreflection studies of single crystal pyrolytic and kish graphite, *Carbon* **11**, 575 (1973).
- [44] Z. Q. Li, S.-W. Tsai, W. J. Padilla, S. V. Dordevic, K. S. Burch, Y. J. Wang, and D. N. Basov, Infrared probe of the anomalous magnetotransport of highly oriented pyrolytic graphite in the extreme quantum limit, *Phys. Rev. B* **74**, 195404 (2006).
- [45] M. L. Sadowski, G. Martinez, M. Potemski, C. Berger, and W. A. de Heer, Landau Level Spectroscopy of Ultrathin Graphite Layers, *Phys. Rev. Lett.* **97**, 266405 (2006).
- [46] S. Kimura, T. Nishi, T. Takahashi, T. Hirono, Y. Ikemoto, T. Moriwaki, and H. Kimura, Infrared spectroscopy under extreme conditions, *Physica B* **329-333**, 1625 (2003).
- [47] T. Moriwaki and Y. Ikemoto, BL43IR at SPring-8 redirected, *Infrared Phys. Tech.* **51**, 400 (2008).
- [48] S. Kimura and H. Okamura, Infrared and Terahertz Spectroscopy of Strongly Correlated Electron Systems under Extreme Conditions, *J. Phys. Soc. Jpn.* **82**, 021004 (2013).
- [49] See the Supplemental Material at (URL to be inserted).
- [50] H. Okamura, Methods for obtaining the optical constants of a material, *Optical Techniques for Solid State Materials Characterization* edited by R. Prasankumar and A. Taylor (CRC, Boca Raton, FL, 2011), Chap. 4.
- [51] To perform KK analysis on a measured  $R(\omega)$ , both ends of  $R(\omega)$  were extrapolated as follows. A constant was smoothly connected to  $R(\omega)$  below 265 meV, since strong periodic oscillations were present there due to multiple internal reflections in the sample. Above 380 meV, an extrapolation was made following the actually measured  $R(\omega)$  in visible and uv ranges [10]. Note that specific details of these extrapolations have only minor effects on the obtained  $\sigma(\omega)$  and do not alter the main results of the present work.
- [52] C. E. P. Villegas A. R. Rocha, and A. Marini, Anomalous Temperature Dependence of the Band Gap in Black Phosphorus, *Nano Lett.* **16**, 5095 (2016).
- [53] These two transitions, corresponding to  $\Delta m_j = \pm 1$ , are allowed with left and right circular polarizations. In our experiment, the incident light had a linear polarization, which can be regarded as a superposition of the two circular polarizations. Therefore, both these transitions may be observed in our experiment.
- [54] E. Carre, L. Sponza, A. Lusson, I. Stenger, E. Gaufres, A. Loiseau, and J. Barjon, Excitons in bulk black phosphorus evidenced by photoluminescence at low temperature, *2D Materials* **8**, 021001 (2021).
- [55] X. Zhou, unpublished work and private communications.
- [56] The results of the quadratic fitting are the following. For X1 peak,  $a = 4.74 \times 10^{-3} \text{ meV/T}^2$ ,  $b = 3.21 \times 10^{-2} \text{ meV/T}$  with  $E_{X1} = 273.0 \text{ meV}$ . For X2 peak,  $a = 9.26 \times 10^{-3} \text{ meV/T}^2$ ,  $b = 1.08 \times 10^{-1} \text{ meV/T}$  with  $E_{X2} = 279.3 \text{ meV}$ .
- [57] R. P. Seisyan, Diamagnetic excitons and exciton magnetopolaritons in semiconductors, *Semicond. Sci. Technol.* **27**, 053001 (2012).
- [58] H. Okamura, D. Heiman, M. Sundaram, and A. C. Gossard, Inhibited recombination of charged magnetoexcitons, *Phys. Rev. B* **58**, R15985 (1998).